Magnetic study of SmCoAsO showing a ferromagnetic-antiferromagnetic transition

Hiroto Ohta,[1,*] Chishiro Michioka,[1] Akira Matsuo,[2] Koichi Kindo,[2] and Kazuyoshi Yoshimura[1,†]

[1]*Department of Chemistry, Graduate School of Science, Kyoto University, Kyoto 606-8502, Japan*
[2]*Institute for Solid State Physics, The University of Tokyo, Kashiwanoha, Kashiwa, Chiba 277-8581, Japan*

We synthesized a polycrystalline sample of SmCoAsO and measured its magnetization (M) at various of temperatures (T) and magnetic fields (H). As decreasing T, a paramagnetic to ferromagnetic transition occurs at 70 K, and then a ferromagnetic to antiferromagnetic transition occurs at 42 K. In the antiferromagnetic phase, we observed the behavior characteristic of metamagnetic transitions in M-H curves. From the results of magnetization measurements up to $H=56$ T, we successfully draw the magnetic phase diagram of SmCoAsO. We observed convex behavior in Arrott plots in the ferromagnetic temperature region as seen in MnSi, $Fe_{1-x}Co_xSi$, and isostructural compound LaCoAsO. We discussed the magnetic property of SmCoAsO above T_C based on the spin-fluctuation theory.

I. INTRODUCTION

Recent discovery of the high-T_c superconductivity in iron pnictides[1,2] has aroused much interest, and many intensive experimental and theoretical studies have been devoted so far to clarifying the superconducting mechanism and to discovering the related new superconducting materials with much higher superconducting transition temperatures (T_c). For the sake of such efforts, several Fe-based compounds, with the same structure as the original compound of LaFeAs(O, F), were found to show the superconductivity with T_c up to 55 K.[3–7] Iron atoms in $LnFePn$O (Ln: lanthanoids, Pn=P and As) can be substituted to other transition metals. Chemical studies on $LnTmPn$O (Tm: transition metals) were first reported by certain German groups,[8] and recently the detailed physical properties were reported by several groups. In the case of Tm=Mn, LaMnPO is an antiferromagnetic semiconductor.[9] In the case of Tm=Ni, LaNiPO is a superconductor with $T_c \sim 2$ K.[10] On the other hand, in the case of Tm=Co, LaCoAsO and LaCoPO are ferromagnets with the Curie temperature (T_C) equal to 50 K and 60 K, respectively.[11–13]

LaCoPnO have a tetragonal crystal structure with the space group of $P4/nmm$ (ZrCuSiAs type), which is the same structure as LaFeAsO (see Fig. 1). In these compounds, cobalt atoms form a two-dimensional (2D) square lattice, which is sandwiched by pnictide layers. LaCoPnO are thus expected to be a ferromagnet with highly 2D ferromagnetic spin fluctuations. We previously analyzed the magnetic property of LaCoAsO on the basis of the self-consistent renormalized (SCR) theory of spin fluctuations[14] and Takahashi's spin-fluctuation theory,[15] and we clarified that three-dimensional (3D) ferromagnetic spin fluctuations are dominant around T_C, and a crossover from the 3D spin fluctuations to the 2D ones occurs at higher temperatures than T_C.[13]

Lanthanum atoms in LaCoPnO can be substituted to other lanthanoid atoms,[16] i.e., Ce, Pr, Nd, Sm, and Gd. We synthesized these compounds and measured their magnetization as a function of temperature (T) and magnetic field (H).[17] All the compounds were found to show ferromagnetic transitions, and the T_C increases from 55 to 70 K with changing La

to Ce and does not change with changing Ce to more heavier lanthanoids. In addition, we discovered ferromagnetic-antiferromagnetic transitions (FAFT) in the cases of Ln=Nd, Sm, and Gd. It can be suggested that the origin of the FAFT is the Ruderman-Kittel-Kasuya-Yoshida interaction, through which localized magnetic moments of $4f$ electrons of Ln^{3+} interact with ferromagnetically ordered magnetic moments of $3d$ itinerant electrons of Co. We showed an evidence of conduction electrons reaching Ln site from the CoAs planes utilizing NMR measurements,[18] which supports the above scenario. We also suggested that the magnetic moments of Co, which interact with each other in CoAs planes, only weakly interact with each other along the c-axis direction, and magnetic properties of LnCoAsO are thus expected to have highly 2D nature. In recent reports on neutron-diffraction measurements,[19,20] the magnetic structure of Nd-CoAsO in the ground state is that the magnetic moments of both Co and Nd^{3+} lie within the ab plane with magnetic moments in neighboring planes heading to opposite directions with each other. Furthermore, an additional magnetic transition was reported at 3.5 K, below the FAFT tempera-
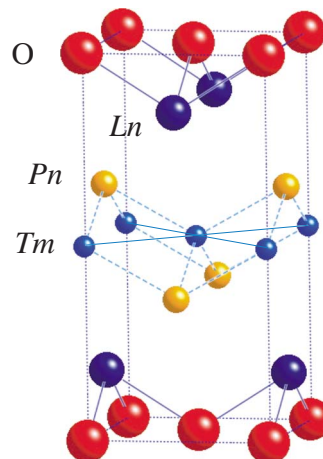

FIG. 1. (Color online) Crystal structure of $LnTmPn$O (Ln: lanthanoids, Tm: transition metals, and Pn: P or As). Space group is $P4/nmm$ (ZrCuSiAs type). SmCoAsO has the same crystal structure (Ln=Sm, Tm=Co, and Pn=As).

ture $T_N = 14$ K, and above this additional transition temperature the antiferromagnetically ordered magnetic moments of Nd^{3+} in the ground state partly become disorder. The other magnetic moments of Nd^{3+} still antiferromagnetically order above 3.5 K together with those of Co and the magnetization of NdCoAsO thus remains small up to $T_N = 14$ K. These results are consistent with our scenario reported in Refs. 17 and 18. Recently, a similar magnetic transition was reported in SmCoAsO at 5 K,[21] at which a peak anomaly was observed in temperature dependence of specific heat as in the same case with NdCoAsO. The magnetic properties of LnCoAsO are so rich and interesting as shown above that these compounds have attracted increasing attentions in these days.

In this paper, we show the detailed magnetic properties of the polycrystalline sample of SmCoAsO, which is a weakly itinerant-electron ferromagnetic compound with the 2D layered crystal structure and shows the FAFT at 42 K. We propose the magnetic phase diagram of SmCoAsO and also show the result of analysis of magnetization based on the SCR theory of spin fluctuations and Takahashi's spin-fluctuation theory with the same manner as in the case with LaCoAsO reported in our previous paper.[13]

II. EXPERIMENTS

In this paper, we used the same polycrystalline sample of SmCoAsO as in Ref. 17 for all the measurements. For the synthesis of a polycrystalline sample of SmCoAsO, we used powders of Sm (purity: 99.9%), As (99.99%), and CoO (99.99%) as starting materials. First, powders of Sm and As were mixed and put in an evacuated silica tube. The mixture of Sm and As was carefully fired at 550 °C for 5 h and then at 800 °C for 12 h. The obtained powder of SmAs was mixed with the powder of CoO to a stoichiometric ratio and ground well in hexane to avoid an oxidation. The pelletized mixture of SmAs and CoO was put in an evacuated silica tube and fired at 1100 °C for 12 h.

Powder x-ray diffractions (PXRDs) were measured for the obtained polycrystalline sample in order to confirm it to be in a single phase of SmCoAsO. As the result, this sample found to contain negligibly small amount of CoAs.[17] Since CoAs is a paramagnetic metal with small magnetic susceptibility, this impurity phase does not affect the results of magnetic measurements below. The lattice parameters a and c were estimated as 3.953 and 8.238 Å (unit-cell volume is 128.729 Å^3), respectively, by PXRD, being in good agreement with the previous reports.[16] Magnetization (M) of SmCoAsO was measured as a function of T and H with the superconducting quantum interference device (SQUID) magnetometer in Research Center for Low Temperature and Materials Sciences, Kyoto University up to 5.5 T and also with the extraction method up to 14 T. Using the SQUID magnetometer, M vs H curves were measured with decreasing H from 5.5 T to zero, and each curve was measured with increasing T from 1.9 K after cooling from room temperature with applying the magnetic field. In the 14 T magnet, M vs H curves were measured with increasing H from 0 to 14 T and then decreasing to zero by sweeping H, and each curve was
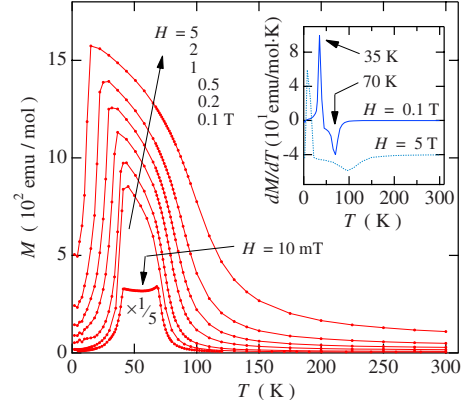

FIG. 2. (Color online) Temperature dependence of M of SmCoAsO at $H = 0.01$ (=10 mT), 0.1, 0.2, 0.5, 1, 2, and 5 T. The data at 10 mT is magnified five times for the good view. Inset: temperature dependence of dM/dT at $H = 0.1$ and 5 T. dM/dH at 5 T is offset along longitudinal axis.

measured with increasing T from 1.9 K after cooling from room temperature with applying the magnetic field. We also measured magnetization in pulsed magnetic fields up to about 56 T carried out with a nondestructive pulsed magnet at 4.2 K at the Institute for Solid State Physics, the University of Tokyo.

III. RESULTS AND DISCUSSION

A. Results of magnetization measurements

Figure 2 shows T dependence of M at $H = 0.1$, 0.2, 0.5, 1, 2, and 5 T. The inset of Fig. 2 shows temperature derivatives of M at $H = 0.1$ and 5 T. The dM/dT at $H = 0.1$ T shows the sharp maximum at 35 K and the minimum at 70 K. This minimum around 70 K broadens with the increase in H. This behavior resembles that of LaCoAsO and the other weakly itinerant ferromagnetic (WIF) compounds around T_C. This indicates that SmCoAsO shows the ferromagnetic transition around 70 K. On the other hand, sharpness of the peak of dM/dT around 35 K does not broaden with the increase in H, and the temperature of the sharp maximum of dM/dT gradually decreases from about 35 to about 20 K with increasing H. Ferromagnetically ordered magnetic moments of Co seem to vanish in the low-temperature region. In our preliminary study of μSR measurements for SmCoAsO, the internal magnetic field is shown to change abruptly below 42 K.[22] This fact and our results of the magnetic measurements show that the transition seen around 35 K is the FAFT. Recently, the evidence of the FAFT is also shown from the results of neutron-diffraction measurements in the case of NdCoAsO,[19,20] which shows a similar sharp drop at about 14 K.[17] The FAFT was, to our knowledge, observed in several systems, e.g., Fe_xRh_{1-x} system,[23] La_2Ni_7,[24] Heusler-type $Ni_{0.5}Mn_{1-x}Si_x$,[25] and CoMnSi.[26] As already reported in Ref. 17, the FAFT was also observed in GdCoAsO with the FAFT temperature (T_N) at low H being about 75 K. The common feature of these compounds seems to have two magnetic sites and one of them has an itinerant electronic nature while the other has a localized electronic one. We also showed the
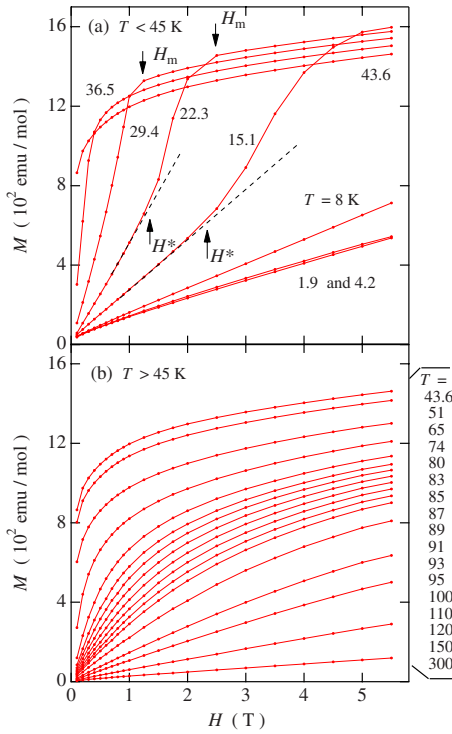
FIG. 3. (Color online) M versus H at various temperatures (a) below and (b) above 45 K. Each curve was measured with decreasing H from 5.5 T after field cooling. Arrows indicate H_m or H^*.

temperature dependence of the M at low H (=10 mT) in Fig. 2. The data shown in the figure was magnified five times for the good view. The M shows two peaks at T_N and T_C as reported in Ref. 21. This result may indicate the existence of antiferromagnetic correlation between T_N and 70 K only in the low-H regions as observed in MnSi.[27]

Figure 3 shows H dependence of M at various T. Between 40 and 70 K, the convex H dependence of M, i.e., the rapid increase in M up to 1 T and then the decrease in the increasing rate of M above 1 T were observed. These behaviors of the M-H curves are quite similar to those of ferromagnetic LaCoAsO below T_C=55 K. Therefore, the ferromagnetic ordered state is again indicated to be realized between 40 and 70 K. On the other hand, below 40 K quite different behaviors of M-H curves have been observed compared to the T region above 40 K. Below 8 K, the M shows a weak H dependence, indicating an antiferromagnetic state is realized. Between 15 and 40 K, the M shows a metamagnetic transition with increasing H. The metamagnetic transition field (H_m) gradually decreases with the increase in T and becomes zero at 36.5 K. The slope of M changes at H=H^* as indicated by arrows. Between H^* and H_m an intermediate state of the metamagnetic transition seems to be realized. The H^* decreases with increasing T in the same way with H_m, and the gap between H^* and H_m becomes smaller with increasing T. The M above H_m seems to naturally connect to that of the ferromagnetic state in the higher T region, indicating that the ferromagnetic state is induced by H in the low-T region.

We also measured the H dependence of M up to higher H to determine H_m below 15 K. Figure 4(a) shows the M-H curves up to 14 T. Below 15 K, metamagnetic transitions
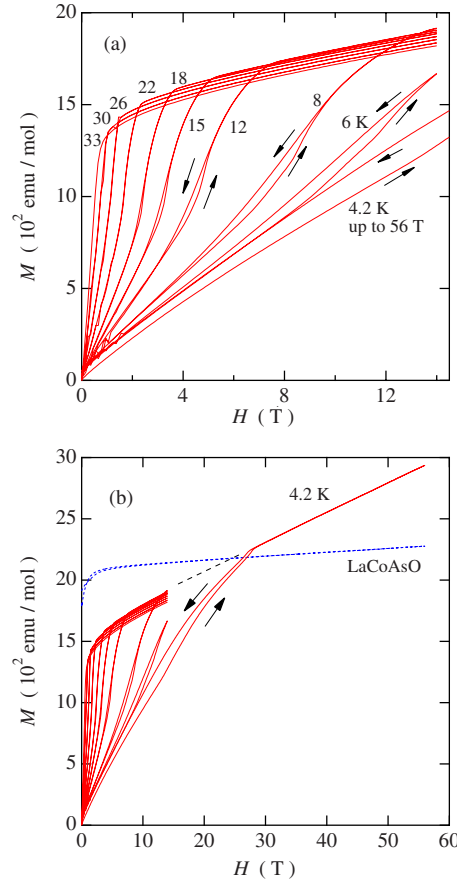

FIG. 4. (Color online) M versus H measured up to 56 T at 4.2 K and up to 14 T at 8, 12, 15, 18, 22, 26, 30, and 34 K. Each curve was measured with increasing and then decreasing H. Dotted line in (b) shows M of LaCoAsO at 4.2 K.

were observed above 5.5 T and the hysteresis was observed below 18 K. The existence of the hysteresis in the M-H curve is the evidence of the H-induced first-order transition which should be the metamagnetic transition. Since Fig. 4(a) shows that 14 T is not high enough to induce the metamagnetic transition below 6 K, we measured M up to 56 T using a strong pulsed magnetic field and the result is shown in Fig. 4(b). At 4.2 K, we successfully observed metamagnetic transition below H_m=28 T below which the hysteresis is observed. Since above H_m no hysteresis was observed at T=4.2 K, all the magnetic moments in the sample are shown to respond completely to the pulsed magnetic field. The dashed line in the figure shows the extrapolation of M above H_m to the low-H region. The natural connection of the dashed line to M in the high-H region above 8 K shows that the electronic state above H_m at 4.2 K is the same as the one above H_m in the higher T. The dotted line in Fig. 4(b) shows M of LaCoAsO at T=4.2 K measured under the strong pulsed magnetic field. This saturating behavior shows that LaCoAsO is not a ferrimagnet or an antiferromagnet but a weakly itinerant-electron ferromagnet. The spontaneous magnetization at the ground state of the ferromagnetic phase, which is roughly estimated by the intersection between the dashed line and the vertical axis, is small compared to that of LaCoAsO in spite of the fact that T_C is higher than La-
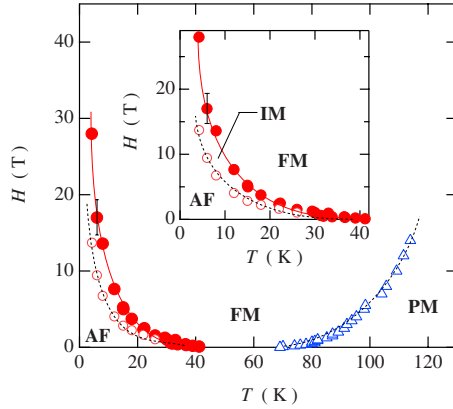
FIG. 5. (Color online) Magnetic phase diagram of SmCoAsO. Open circles, closed circles, and open triangles stand for the H^*, T_N, and T_C, respectively (see text). AF, FM, PM, and IM denote antiferromagnetic, ferromagnetic, paramagnetic phases, and an intermediate state, respectively. Solid and dotted lines are guides for the eyes. $T_N = 42$ K at $H = 0$.

CoAsO, indicating the difference in the spin-fluctuation spectrum or the shrinkage of ordered magnetic moments. The M of LaCoAsO shows the saturation behavior above 1 T while in the case of SmCoAsO the M continues to increase in the high-H ferromagnetic region. Since the magnetic moments of Co are thought to be saturated in the high-H region, the increase in M against H can be attributed to the paramagnetic or spin-flopping localized magnetic moments of $4f$ electrons of Sm^{3+} ions.

From the data in Figs. 2–4, we estimated the Curie temperature T_C and the FAFT temperature T_N at various H, and the results are shown in Fig. 5. Here, the inset shows the magnification of a part of the main panel. As shown in the figure, the T_N at $H = 0$ is about 42 K. The labels AF, FM, PM, and IM denote the antiferromagnetic, the ferromagnetic, the paramagnetic phases, and the intermediate state, respectively. Open circles stand for H^* at which the M starts to deviate from the linear line in the low-H region when H is increased. Closed circles stand for T_N (or H_m). Open triangles stand for T_C which is estimated as the peak temperature of dM/dT at $H \neq 0$ and the estimated T_C from the results of the Arrott plots at $H = 0$. Below H^*, the antiferromagnetic state is realized while above H_m the ferromagnetic state is realized. The magnetic phase diagram of SmCoAsO quite resembles that of CoMnSi$_{1-x}$Ge$_x$ reported recently,[28] though we did not observe the two step metamagnetic transitions seen in CoMnSi$_{1-x}$Ge$_x$. The magnetic phase diagrams of two compounds indicates that the mechanism of FAFT is similar with each other and the localized moments of Sm in SmCoAsO seem to correspond to magnetic moments of Mn in CoMnSi. Theoretical studies about FAFT in the itinerant electronic systems were reported by Moriya and Usami[29] and Isoda.[30] At first, Moriya and Usami discussed situations to occur the FAFT based on the Landau expansion of free energy with the susceptibility χ_q^0 which has double peaks at $q = 0$ and Q. According to them, SmCoAsO (and CoMnSi) corresponds to the situation of (I-2) in their report with T^* being zero, however the curve of FAFT field against temperature is different from our case. We showed the H dependence of T_C in Fig. 5,
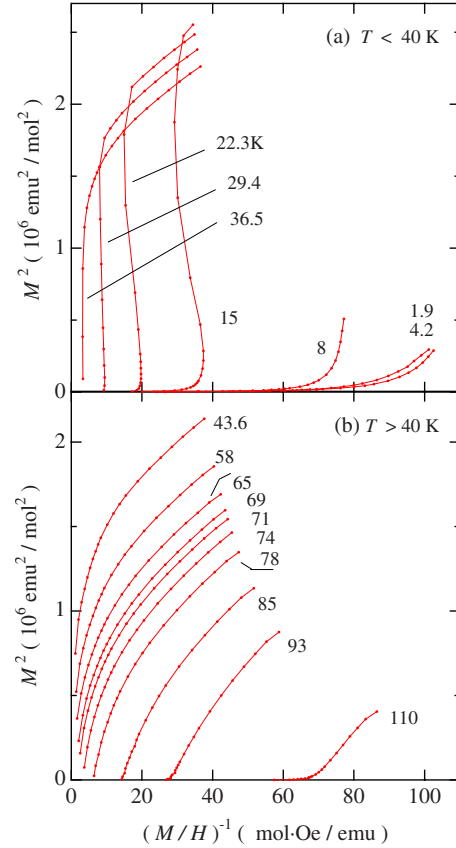

FIG. 6. (Color online) M^2 versus H/M at various temperature (a) below and (b) above 40 K.

in which the T_C is determined as the local minimum of the dM/dT against T. As seen in Fig. 2, the peak of the dM/dT around T_C is more broadened with increasing H, indicating that the boundary between paramagnetic and ferromagnetic phases vanishes in the high-field region. Such a feature quite resembles the supercritical point of water. Above the critical point between paramagnetic and ferromagnetic phases, we can not distinguish the ferromagnetically ordered state and the forced ferromagnetic state by H just as the case with the supercritical phenomena in water, although such a supercritical point was not observed up to 14 T in this compound.

B. Analyses of magnetization

For the analyses of the magnetic properties in the ferromagnetic and paramagnetic states of SmCoAsO, we replotted the M-H curves in the forms of M^2 versus H/M, so-called Arrott plots. Typical weakly itinerant-electron ferromagnets such as ZrZn$_2$, Sc$_3$In, and Ni$_3$Al show the linear relation between M^2 and H/M at and around T_C, and the T_C can be determined as the temperature at which the extrapolation of M^2 against H/M passes the origin. Figure 6 shows the M^2 versus H/M plots (a) below and (b) above 40 K. In all the T region, the M^2 does not obey the linear relation against H/M. Below 40 K, the M^2 shows an "S" like behavior because of the metamagnetic transition. In the previous report, we showed that the M^2 of LaCoAsO shows a convex behavior against H/M at and around T_C (Ref. 13) as
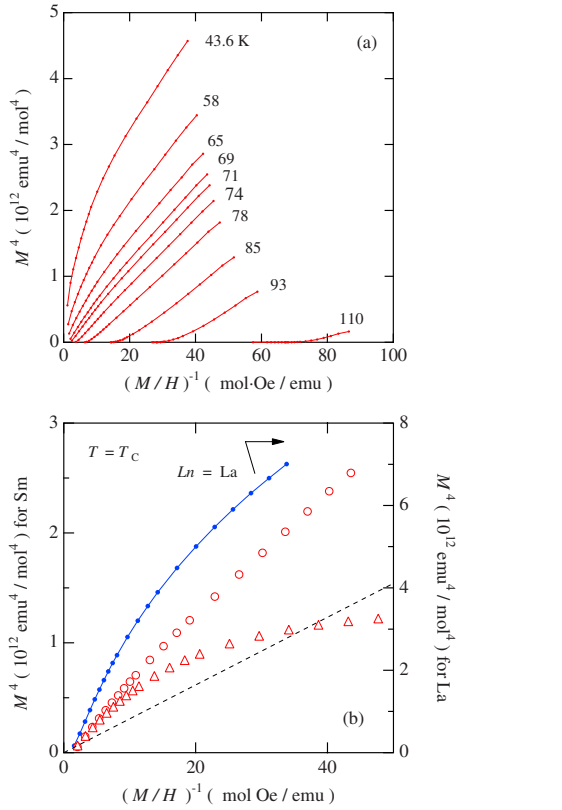
FIG. 7. (Color online) (a) M^4 versus H/M at various temperature. (b) M^4 vs H/M at 69 K (open circles) together with that of LaCoAsO at T_C (closed circles). Open triangles show M of Co (see text). Dashed line shows a result of linear fit to M of Co.

seen in MnSi (Ref. 27) and $Fe_{1-x}Co_xSi$.[31] As shown in Fig. 6(b), the M^2 of SmCoAsO shows the convex behavior above 40 K, similar to that of LaCoAsO, especially around T_C (~ 70 K). This indicates that in SmCoAsO the quite similar electronic state is realized as in the case with LaCoAsO. The M of MnSi and $Fe_{1-x}Co_xSi$ was reported to show the linear relation in the form of M^4 versus H/M plot,[15,31] which was predicted by Takahashi in his spin-fluctuation theory.[15] We also showed in our report that the M of LaCoAsO obeys the linear relation in the M^4 versus H/M plot. Figure 7(a) shows the M^4 versus H/M plots of SmCoAsO above 40 K. The M of SmCoAsO also shows the linear relation between M^4 and H/M at and around T_C. Figure 7(b) shows the data at T_C, where the M^4 obeys almost perfect linear relation against H/M. We also shows Arrott plots and the M^4 versus H/M plots for the data measured under high H below 40 K in Fig. 8.

We estimated the spontaneous magnetization (M_s) below T_C and the reciprocal magnetic susceptibility (χ^{-1}) (=$\lim_{H\to 0} H/M$) above T_C from the Arrott plot (Fig. 6) as the values of the intersections of natural extrapolations of the M^2-H/M curves with the vertical and horizontal axes, respectively, and showed the T dependence of them in Fig. 9. Since the M_s can not be obtained in this method below 40 K, we estimated the spontaneous magnetization in the ground state (P_s) [=$M_s(0)$] from the natural extrapolation to the vertical axis, and obtained P_s as 909 emu/mol or 0.163 μ_B. From the T dependence of χ^{-1} we estimated the effective
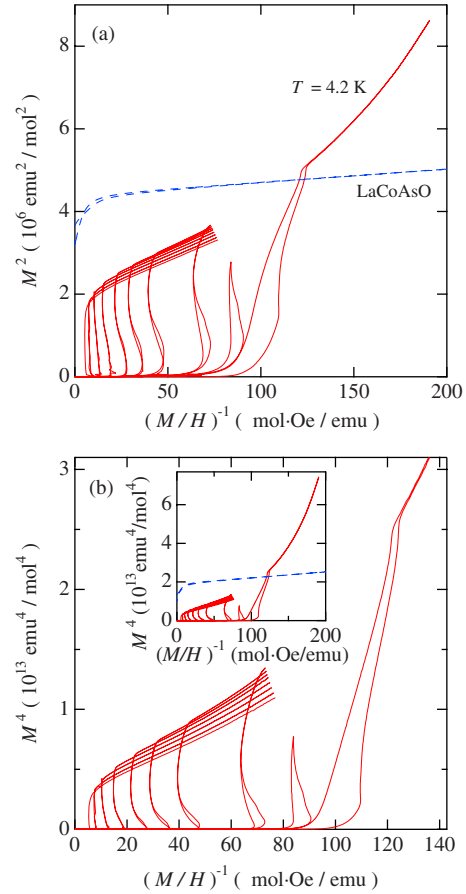

FIG. 8. (Color online) (a) M^2 and (b) M^4 versus H/M under high H. Dotted lines in (a) and inset of (b) show the data of LaCoAsO.

Bohr magneton number (P_{eff}). Since SmCoAsO has both the itinerant magnetic moments derived from $3d$ electrons of Co and the localized magnetic moments derived from $4f$ electrons of Sm^{3+} ions, we tried to fit the following function to the χ:
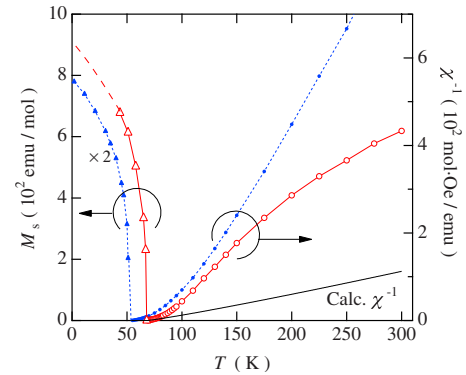

FIG. 9. (Color online) T dependences of M_s and χ^{-1} of Sm-CoAsO. Closed symbols with dotted line show $M_s/2$ and χ^{-1} of LaCoAsO. Dashed line shows the natural extrapolation of M_s to longitudinal axis. Solid line shows the calculated χ^{-1} based on the SCR theory of spin fluctuations (Refs. 14 and 33).

TABLE I. Parameters estimated from a fitting of Eq. (1) to χ^{-1} together with those of LaCoAsO for the comparison. θ_{Sm} was fixed to 42 K.

Ln	P_{eff} (μ_B)	θ_{Co} (K)
Sm	1.68	78.9
La	1.34	98.4

$$f(T) = \frac{C_{Co}}{T - \theta_{Co}} + \frac{C_{Sm}}{T - \theta_{Sm}}, \qquad (1)$$

where C_i and θ_i are the Curie constant ($=NP_{eff,i}^2\mu_B^2/3k_B$) and the Weiss temperature for i equal to Co and Sm, respectively. We assumed the T-independent part of χ to be zero. For the fitting, we used P_{eff} of Sm^{3+}, which is obtained as a function of T from the calculation considering the multiplet terms of $^6H_{7/2}$ and $^6H_{9/2}$ whose centers of gravity are about 1500 and 3250 K compared with the lowest multiplet term of $^6H_{5/2}$ by referring the case of paramagnetic Sm^{3+} in $LaCl_3$ (Ref. 32) and by assuming the crystal field is negligibly small. The fitting result was listed in Table I together with those of LaCoAsO. The M shown in Sec. III A also contains two components, i.e., one derived from $3d$ electrons of Co and another $4f$ electrons of Sm. The value of P_{eff} seems valid comparing with that of LaCoAsO, showing that we successfully separated the magnetism of Co and Sm. For the analysis of the magnetic property of conduction electrons in CoAs in the next paragraph, we tried to subtract the M of Sm^{3+} from the observed M at $T_C = 69$ K. From the above parameters the χ of Sm^{3+} becomes 3.30×10^{-3} emu/mol at 69 K. By subtracting the M of Sm calculated from the χ, we estimated the M of Co and the result is shown in Fig. 7(b) as open triangles. The modified M^4 against H/M shows almost linear behavior, which is similar to that of LaCoAsO. We analyzed the magnetic properties of the ferromagnetic and paramagnetic states of SmCoAsO on the basis of the SCR theory of spin fluctuations[14] and Takahashi's spin-fluctuation theory.[15]

According to the theory of the spin fluctuation by Takahashi,[15] it was assumed that the sum of zero point and thermal spin fluctuations is conserved against T, and as the consequence of this assumption he argued the importance of the sixth coefficient of the free energy when the system has a relatively larger $\eta[=(T_C/T_0)^{1/3}]$ value. Here T_0 characterizes the energy width of the dynamical spin-fluctuation spectrum. In such case, the magnetization obeys following relation at T_C because the fourth coefficient becomes zero:

$$h = [T_A/3(2 + \sqrt{5})T_C]^2 p^5, \qquad (2)$$

where $h/2\mu_B$ and p are the magnetic field and the magnetization in μ_B unit, respectively. Therefore, M^4 comes to be linear against H/M. We showed in the previous paper that the M of LaCoAsO obeys such the linear relation between M^4 and H/M, and obtained spin-fluctuation parameter T_A from the slope of it.[13] We obtained T_A by putting the value of the slope of the M^4 against H/M at T_C into the following equation:

$$M^4 = 1.17 \times 10^{19}(T_C^2/T_A^3)(H/M), \qquad (3)$$

where M and H are in emu/mol and Oe units, respectively. The estimated value of T_A was 12.2×10^3 K. According to the SCR theory for WIF,[14,33,34] T_C is related with P_s, T_A, and T_0 as a following relation:

$$T_C = (60c)^{-3/4}P_s^{3/2}T_A^{3/4}T_0^{1/4}, \qquad (4)$$

where c is a constant equal to 0.3353… By putting the value of T_A determined by Eq. (5), we obtained T_0 as 5.45×10^3 K. We estimated $\bar{F}_1$ from the following relation:

$$\bar{F}_1 = 4T_A^2/15T_0. \qquad (5)$$

This relation was predicted in Takahashi's theory.[15] By putting the obtained values of T_A and T_0 to Eq. (7), the value of $\bar{F}_1$ becomes 7.28×10^3 K. The estimated spin fluctuation and the thermodynamic parameters are listed in Table II together with those of LaCoAsO for the comparison.

Using the spin fluctuation and the thermodynamic parameters, one can calculate the $1/\chi$ in a paramagnetic state by the SCR theory as

$$y \approx \bar{f}_1\left(-1 + \frac{1 + \nu y}{c}\int_0^{1/\eta} dzz^3\left[\ln u - \frac{1}{2u} - \Psi(u)\right]\right) \quad (6)$$

with $y^{-1} = 4\eta^2 T_A\chi/3$, $u = z(y + z^2)/t$, $\eta = (T_C/T_0)^{1/3}$, $\bar{f}_1 = \bar{F}_1 P_s^2/8T_A\eta^2$, $\nu = \eta^2 T_A/U$, $c = 0.3353…$, where $\Psi(u)$ is the digamma function, $t = T/T_C$ and U the intra-atomic exchange energy ($\sim 10^4$ K). The detailed calculation method was described in Refs. 15 and 33–35. The calculated χ^{-1} is shown in Fig. 9 as the solid line. There is a large difference between the experimental and calculate χ's as seen in the figure. The value of P_{eff} of the calculated χ around 300 K is about 3.9 μ_B, which is about 2.3 times larger than that of the experimental one.

To see the validity of the obtained spin fluctuation and thermodynamic parameters, we plotted the P_{eff}/P_s against the T_C/T_0 on the so-called generalized Rhodes-Wohlfarth plot[36,37] as seen in Fig. 10. SmCoAsO can be plotted as the

TABLE II. Spin-fluctuation parameters of SmCoAsO together with LaCoAsO for the comparison.

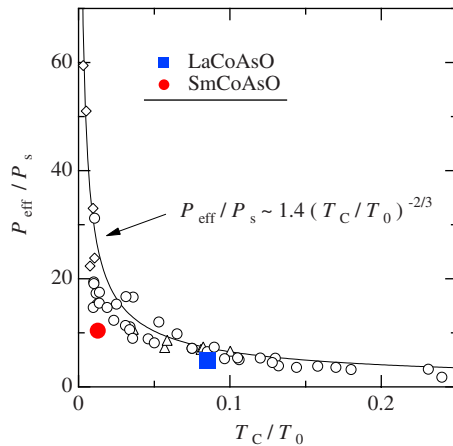|	T_C (K)	T_A (10^3 K)	T_0 (10^3 K)	$\bar{F}_1$ (10^3 K)	P_s (μ_B)
Sm	69	12.2	5.45	7.28	0.163
La	55	6.21	0.64	16.0	0.28

FIG. 10. (Color online) Generalized Rhodes-Wohlfarth plot. SmCoAsO can be plotted as a closed circle. Closed square shows LaCoAsO (Ref. 13). Open symbols are the data reproduced from Refs. 15, 30, and 34–36.

closed circle which is rather far from the theoretical line of $P_{eff}/P_s \sim 1.4(T_C/T_0)^{-2/3}$.[15] The closed square shows LaCoAsO.[13] According to Takahashi, when the quasi-two-dimensionality is introduced into the spin-fluctuation theory, the theoretical curve of P_{eff}/P_s as a function of T_C/T_0 is gradually reduced with decreasing the two-dimensional parameter ϵ ($\equiv \sqrt{m_{a,b}/m_c}$, m_i is mass of conduction electrons along i axis).[38] Therefore, the smaller value of P_{eff}/P_s in SmCoAsO (and also in LaCoAsO) comparing to the theoretical value may indicate the high two-dimensional nature of spin fluctuations in CoAs planes. It should be noted, however, that throughout the analyses in this section we took in mainly two assumption: the crystal field at Sm site is negligibly small, and the correlation between $3d$ electrons of Co and $4f$ electrons of Sm^{3+} is not explicitly concerned. Therefore, our suggestion about the two dimensionality is not be-

yond speculation. To clarify the difference between the estimated value and theoretical curve, analyses completely based on the quasi-two-dimensional spin-fluctuation theory are needed. It is also important to cross-check the parameters of spin fluctuations using neutron-diffraction and/or NMR measurements.

IV. CONCLUSION

We studied the detailed magnetic property of a polycrystalline sample of SmCoAsO through the magnetic measurements under various magnetic fields up to 56 T. From the measurements we successfully drew the magnetic phase diagram of SmCoAsO, where antiferromagnetically ordered phase is separated from the ferromagnetically ordered phase by the hyperbolic line as seen in $CoMnSi_{1-x}Ge_x$. We analyzed magnetization from the view point of the spin-fluctuation theory. Although we carefully subtracted the magnetization derived from Sm^{3+} from the observed data and estimated the spin-fluctuation parameters by fitting the theoretical function to the data, the calculated magnetic susceptibility using estimated parameters did not fit to the experimental one. This possibly indicates that spin fluctuations in the CoAs plane are not three dimensional but quasi-two-dimensional in the high-temperature region.

*shioshio@kuchem.kyoto-u.ac.jp

†kyhv@kuchem.kyoto-u.ac.jp

[1] Y. Kamihara, H. Hiramatsu, M. Hirano, R. Kawamura, H. Yanagi, T. Kamiya, and H. Hosono, J. Am. Chem. Soc. **128**, 10012 (2006).

[2] Y. Kamihara, T. Watanabe, M. Hirano, and H. Hosono, J. Am. Chem. Soc. **130**, 3296 (2008).

[3] Z. A. Ren, J. Yang, W. Lu, W. Yi, X. L. Shen, Z. C. Li, G. C. Che, X. L. Dong, L. L. Sun, F. Zhou, and Z. X. Zhao, EPL **82**, 57002 (2008).

[4] M. Rotter, M. Tegel, and D. Johrendt, Phys. Rev. Lett. **101**, 107006 (2008).

[5] F. C. Hsu, T. Y. Luo, K. W. Yeh, T. K. Chen, T. W. Huang, P. M. Wu, Y. C. Lee, Y. L. Huang, Y. Y. Chu, D. C. Yan, and M. K. Wu, Proc. Natl. Acad. Sci. U.S.A. **105**, 14262 (2008).

[6] X. C. Wang, Q. Q. Liu, Y. X. Lv, W. B. Gao, L. X. Yang, R. C. Yu, F. Y. Li, and C. Q. Jin, Solid State Commun. **148**, 538 (2008).

[7] H. Ogino, Y. Matsumura, Y. Katsura, K. Ushiyama, S. Horii, K.

Kishio, and J. Shimoyama, Supercond. Sci. Technol. **22**, 075008 (2009).

[8] For example, B. I. Zimmer, W. Jeitschko, J. H. Albering, R. Glaum, and M. Reehuis, J. Alloys Compd. **229**, 238 (1995), and references therein.

[9] A. T. Nientiedt, W. Jeitschko, P. G. Pollmeier, and M. Brylak, Z. Naturforsch. **52b**, 560 (1997).

[10] T. Watanabe, H. Yanagi, T. Kamiya, Y. Kamihara, H. Hiramatsu, M. Hirano, and H. Hosono, Inorg. Chem. **46**, 7719 (2007).

[11] H. Yanagi, R. Kawamura, T. Kamiya, Y. Kamihara, M. Hirano, T. Nakamura, H. Osawa, and H. Hosono, Phys. Rev. B **77**, 224431 (2008).

[12] A. S. Sefat, A. Huq, M. A. McGuire, R. Jin, B. C. Sales, D. Mandrus, L. M. D. Cranswick, P. W. Stephens, and K. H. Stone, Phys. Rev. B **78**, 104505 (2008).

[13] H. Ohta and K. Yoshimura, Phys. Rev. B **79**, 184407 (2009).

[14] T. Moriya and A. Kawabata, J. Phys. Soc. Jpn. **34**, 639 (1973); **35**, 669 (1973).

[15] Y. Takahashi, J. Phys. Soc. Jpn. **55**, 3553 (1986).

[16] P. Quebe, L. T. Terbüchte, and W. Jeischko, J. Alloys Compd. **302**, 70 (2000).

[17] H. Ohta and K. Yoshimura, Phys. Rev. B **80**, 184409 (2009).

[18] H. Ohta, C. Michioka, and K. Yoshimura, J. Phys. Soc. Jpn. **79**, 054703 (2010).

[19] M. A. McGuire, D. J. Gout, V. O. Garlea, A. S. Sefat, B. C. Sales, and D. Mandrus, Phys. Rev. B **81**, 104405 (2010).

[20] A. Marcinkova, D. A. M. Grist, I. Margiolaki, T. C. Hansen, S. Margadonna, and Jan-Willem G. Bos, Phys. Rev. B **81**, 064511 (2010).

[21] V. P. S. Awana, I. Nowik, A. Pal, K. Yamaura, E. Takayama-Muromachi, and I. Felner, Phys. Rev. B **81**, 212501 (2010).

[22] J. Sugiyama *et al.* (private communication).

[23] M. Fallot and R. Hocart, Rev. Sci. Instrum. **77**, 498 (1939).

[24] M. Fukase, Y. Tazuke, H. Mitamura, T. Goto, and T. Sato, J. Phys. Soc. Jpn. **68**, 1460 (1999).

[25] T. Krenke, Y. Duman, M. Acet, E. F. Wassermann, X. Moya, L. Mañosa, and A. Planes, Nature Mater. **4**, 450 (2005).

[26] S. Niziol, H. Bińczycka, A. Szytula, J. Todorović, R. Fruchart, J. P. Senateur, and D. Fruchart, Phys. Status Solidi A **45**, 591 (1978).

[27] D. Bloch, J. Voiron, V. Jaccarino, and J. H. Wernick, Phys. Lett. **51A**, 259 (1975).

[28] K. G. Sandeman, R. Daou, S. Özcan, J. H. Durrell, N. D. Mathur, and D. J. Fray, Phys. Rev. B **74**, 224436 (2006).

[29] T. Moriya and K. Usami, Solid State Commun. **23**, 935 (1977).

[30] M. Isoda, J. Magn. Magn. Mater. **27**, 235 (1982).

[31] K. Shimizu, H. Maruyama, H. Yamazaki, and H. Watanabe, J. Phys. Soc. Jpn. **59**, 305 (1990).

[32] J. D. Axe and G. H. Dieke, J. Phys. Chem. **37**, 2364 (1962).

[33] Y. Takahashi and T. Moriya, J. Phys. Soc. Jpn. **54**, 1592 (1985).

[34] T. Moriya, *Spin Fluctuations in Itinerant Electron Magnetism* (Springer-Verlag, New York, 1985).

[35] K. Yoshimura, M. Takigawa, Y. Takahashi, H. Yasuoka, and Y. Nakamura, J. Phys. Soc. Jpn. **56**, 1138 (1987).

[36] Rhodes-Wohlfarth plot was originally reported in P. R. Rhodes and E. P. Wohlfarth, Proc. R. Soc. London **273**, 247 (1963); and E. P. Wohlfarth, J. Magn. Magn. Mater. **7**, 113 (1978). The generalized Rhodes-Wohlfarth plot was reported by Takahashi (Ref. 15).

[37] R. Nakabayashi, Y. Tazuke, and S. Murayama, J. Phys. Soc. Jpn. **61**, 774 (1992).

[38] Y. Takahashi, J. Phys.: Condens. Matter **9**, 10359 (1997).